

Pore structure evolution in silica gel during aging/drying

I. Temporal and thermal aging

Pamela J. Davis^a, C. Jeffrey Brinker^{a,b} and Douglas M. Smith^{a,1}

^a UNM/NSF Center for Micro-Engineered Ceramics, University of New Mexico, Albuquerque, NM 87131, USA

^b Division 1846, Sandia National Laboratories, Albuquerque, NM 87185, USA

Received 16 May 1991

Revised manuscript received 11 November 1991

Low field NMR spin–lattice relaxation measurements of pore fluids contained in silica gels are employed as a pore structure probe to ascertain the changes that occur in a two-step acid/base-catalyzed silica gel during aging in its mother liquor. It has been shown that both a narrowing of pore size distribution and an increase in mean pore size is obtained for a gel aged at 303 K over a time period of several weeks. By increasing the aging temperature from 303 to 333 K, the time required for this same degree of pore size distribution narrowing is decreased by an order of magnitude. Increasing the gel solids content from 15 to 30 wt% SiO₂ results in smaller pore sizes and pore volumes (a factor of ~2) but a similar pore size narrowing with comparable kinetics. In contrast, little change in pore structure is observed in a two-step acid-catalyzed gel aged in its mother liquor at 303 K for similar time periods.

1. Introduction

A major feature of sol–gel processing of ceramics and glasses is the large degree of variation in pore structure (i.e., mean pore size, pore size distribution, surface area, porosity, etc.) that may be achieved during processing. Pore structure control is of great practical interest, since the pore size and size distribution play important roles in fixing the highest evaporation rate that can be achieved without cracking during drying, the sintering temperature, and such physical properties as the refractive index. By varying process parameters such as temperature, pore solvent, pH, aging time, etc., changes in the pore structure may be realized. After the gel point the structure and properties of a gel continue to change. This process is called aging and the changes are dependent on the environment to

which the gel is exposed. There is an extensive literature on aging of silica which is reviewed by Iler [1] and Brinker and Scherer [2]. However, there is little knowledge of the quantitative effect of aging conditions on pore structure, especially in the wet state. Three processes can occur during aging: condensation, coarsening and/or phase transformation [2]. Each of these aging phenomena will be affected by solvent type, aging time, pH and temperature.

At the gel point, the Si–O–Si network has developed sufficiently to prevent flow of the solvent, but many Si atoms still have –OR and –OH groups bonded to them and not all silicate species are attached to the spanning cluster. During aging, terminal Si–OR and Si–OH groups will continue to condense to form SiOSi plus either ROH or H₂O by-products. If low molecular weight species attach to the macromolecule, little volume change of the gel will occur. If terminal –OR and –OH groups condense, the gel matrix is pulled in on itself and shrinkage will occur result-

¹ Author to whom comments should be addressed.

ing in expulsion of pore fluid and an increase in the skeletal density of the solid matrix. This phenomenon is called syneresis and its rate is a function of gel stiffness and permeability, and hence, pore size [3]. Hench and West [4] state that the syneresis rate should increase with solids content and temperature, and that hydrogen bonding of organic solvents inhibits condensation, thus slowing syneresis. Scherer [5] observed that smaller gels shrink faster due to shorter flow paths and that the shape of the shrinkage curves depended upon the gel's permeability and viscoelastic properties. The total syneresis strain was found to be greater at lower temperatures although the contraction rate is less [6]. We suggest that higher temperature promotes condensation reactions that stiffen the matrix, thus retarding gel shrinkage. Vysotskii and co-workers [7,8] have shown gel shrinkage as a function of pH to be minimized at the isoelectric point, at which the condensation rate is minimized. However, the pH also causes changes in gel stiffness and permeability so a direct correlation between pH and syneresis cannot be drawn.

Coarsening or Ostwald ripening is discussed in detail by Iler [1]. In general convex surfaces are more soluble than concave surfaces and dissolved material will tend to be removed from convex surfaces and precipitate into regions of negative curvature. This effect should enhance neck formation between particles and fill small pores thus increasing the average pore size, decreasing specific surface area and increasing matrix strength. Coarsening is favored by conditions of pH and temperature for which the dissolution rate and solubility are high.

Phase transformation may occur due to a phase separation in which polymer clusters form surrounded by regions of free fluid. This process, called 'microsyneresis', occurs when the polymer has a greater affinity for itself than the pore fluid. Microsyneresis was noted by Quinson and co-workers [9] as the cause of large changes in pore size in titania wet gels when placed in different solvents even though the macroscopic gel dimension did not change. Phase separation of unreacted or partially reacted silicon alkoxides has been suggested and observed for a two-step

acid-base-catalyzed process. It caused the gel to turn white and opaque when placed in water [10,11]. Other phase transformations may occur involving crystallization [2] but these are not relevant for the alkoxide-derived silica gels to be studied in this work.

Usually, the effect of processing parameters on wet gel structure and on structural changes during aging and drying is inferred from the pore structure of the final dried gel. However, recent advances in non-intrusive NMR-based pore structure analysis techniques allow the continuous measurement of wet gel pore structure parameters during aging and drying. The ability to monitor pore structure changes throughout aging and drying of sol-gels is complicated since fluids and impurities are contained within the structure. Traditional pore structure analysis methods such as gas sorption and mercury porosimetry must be conducted on dried samples. Typically, structural changes occurring during aging and drying have been inferred from information obtained on dried gels. The few studies that have monitored pore structure evolution during sol-gel aging and drying are based on small-angle scattering (SAXS, SANS), thermoporometry, magnetic resonance imaging (MRI), and/or low-field NMR spin-lattice relaxation.

Scattering has primarily provided information on size and structure of polymeric or particulate species prior to gelation and the structure of dried gels [2]. The use of scattering for in situ pore structure analysis suffers from limited length scales, contrast problems, the relation of scattering results to pore size, multiple scattering and errors resulting from desmearing. However, the approach is quick, allows extraction of all length scales at once, and accesses closed porosity.

Thermoporometry provides pore size information from comparison of melting and solidification thermograms [12]. This technique requires that the sample temperature be slowly varied and relates the change in pore fluid freezing point to pore size for pores in the range of 1 to ~ 100 nm. However, special care must be taken to ensure that the pore fluid is pure and this may significantly change the physical and chemical structure of the gel before analysis as well as limit the types

of pore fluid which may be used. Questions also exist regarding the effect of solidification and melting on gel structure. Quinson and co-workers successfully applied thermoporometry to obtain pore structure information for titania [9] and silica gels [13].

NMR spin–lattice relaxation measurements have also been employed as a tool for analyzing the pore structure of wet solids [14,15]. This technique is well suited for in situ studies of gels as it is a non-intrusive probe of the pore fluid. Pore size and surface area information may be obtained by surface enhanced spin–lattice relaxation measurements of pore fluid. Fluid in the close proximity of a pore surface (< 0.5 nm) will undergo both spin–lattice relaxation (T_1) and spin–spin relaxation (T_2) at a greater rate than the bulk fluid. When diffusion between this surface-affected phase and the bulk pore fluid is fast compared to relaxation, one observes a weighted relaxation time for the pore fluid which is a function of the pore volume to surface area ratio. Glaves and co-workers [16] have used this technique to monitor pore structure evolution during aging and drying of two two-step acid–base-catalyzed silica gel samples aged in either ethanol or ethanol/KOH solutions. They found that gel surface area remained essentially constant during drying until the last several percent of solvent loss when presumably high capillary pressure lead to a dramatic surface area decrease. The magnitude of this surface area decrease was a strong function of pore fluid pH. Recently, Ewing and co-workers [17] have combined MRI and spin–lattice relaxation measurements to obtain the spatial distribution of porosity and the spatially averaged pore size distribution in a single silica gel throughout the drying process.

Although the general effects of time and temperature on aging reactions such as polymerization/condensation are known, how these parameters relate to pore structure have not been well studied. In this work, we study the effect of temporal and thermal aging on the pore structure of silica gels and the resulting dried gels (xerogels). In subsequent work, we will describe the effects of pore fluid composition, pH and surface tension on pore structure.

2. Experimental procedure

Two sets of silica gels were prepared via a two-step procedure employing base catalysis for the second step. Complete details of the gel synthesis are described by Brinker et al. [18] for the first set and the other by a slightly modified process to increase the solids content of the sol. For both sets, the first step consisted of combining tetraethylorthosilicate (TEOS), ethanol, water and HCl (molar ratios 1 : 3 : 1 : 0.0007) and heating under constant reflux at ~ 333 K for 1.5 h. For more concentrated gels, solvent was evaporated in a rotovac to double the solids content (from 15 to 30 wt% SiO_2 , on a final wet gel basis). The mixtures were then gelled by addition of 1 part by volume 0.05M NH_4OH to 10 parts of the stock solution. Two samples of each gel were obtained, and one of each solids content was aged at 303 K and one of each at 333 K (providing 4 samples in all). These gels are denoted as 15 and 30 wt% B2. Samples aged at 333 K were quenched to 303 K for NMR analysis and returned to 333 K immediately after experimentation was completed. For comparison, a similar two-step acid-catalyzed silica gel (denoted as A2) was prepared by gelling the same TEOS stock solution as used above with 1M HCl (0.16 part by volume 1M HCl to 1 part stock solution) at ~ 323 K for 48 h and then aging at 303 K.

Prior to gelation, spin–lattice relaxation created by growth of polysiloxanes was monitored in the 15 wt% sample by equilibrating the precursor sol at 303 K and dispensing it in a 5 mm glass NMR tube. Gelation is a slightly exothermic process and T_1 is sensitive to temperature. However, the measured temperature rise during gelation was found to be insignificant (< 0.1 K).

NMR measurements were performed at a proton Larmor frequency of 20 MHz using a Spin-lock CPS-2 pulse NMR. Data acquisition of the free induction decay (FID) was accomplished via a Hitachi 6431 oscilloscope interfaced with an IBM CS-9000 computer. Spin–lattice relaxation measurements were conducted using a $180^\circ\text{--}\tau\text{--}90^\circ$ pulse sequence. The delay between pulses, τ , was varied non-uniformly from 100 μs to 9 s to obtain approximately 30 $M(\tau)$ points. The distribution

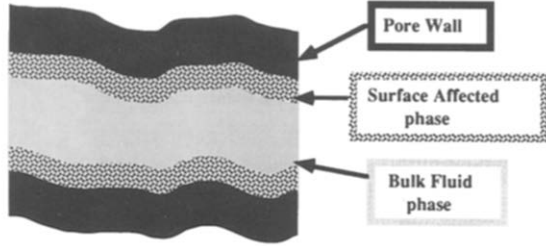


Fig. 1. Schematic diagram of pore fluid during an NMR experiment.

of relaxation times was calculated from $M(\tau)$ using the method of regularization described by Gallegos and Smith [19]. To relate T_1 to pore size, the ‘two-fraction fast-exchange’ model [20] was employed (see fig. 1). This assumes that diffusion between fluid in the close proximity of the surface to bulk fluid is fast as compared to relaxation. From the two-fraction, fast exchange model, the measured T_1 is related to the pore size by [14]

$$\frac{1}{T_1} = \frac{1}{T_{1b}} + \frac{\beta}{r_p}, \quad (1)$$

where the pore size, r_p , is the pore hydraulic radius ($2000 V_p/SA$) in nanometers, V_p is the specific pore volume (cm^3/g), SA is the specific surface area (m^2/g), β is the NMR surface interaction parameter (nm/s), and T_{1b} is the spin–lattice relaxation time of the bulk fluid. When the pore volume is large compared to the surface area (i.e., for pores larger than 3–5 nm), the volume of the surface-affected phase is small and the pore volume to surface area ratio is obtained directly from eq. (1). For smaller pores, assumptions concerning pore geometry and the thickness of the surface-affected phase are required [21]. The thickness of this surface-affected phase is typically 0.3 ± 0.1 nm. The value of β was found by performing relaxation experiments on partially saturated samples [21]. Previously, we have found that both ethanol and water have very similar β and T_{1b} values at these low magnetic fields and no special precautions were deemed necessary despite the fact that the mother liquor is a mixture of ethanol and water (9/1 volume ratio [22]).

In addition to pore size distributions, the specific surface area of wet materials may be extracted from the average spin–lattice relaxation time [23]. The difference between the inverse average relaxation time and the inverse relaxation time of bulk fluid is inversely proportional to surface area multiplied by the solid mass to fluid volume ratio:

$$\frac{1}{T_{1\text{avg}}} - \frac{1}{T_{1b}} = \frac{\beta SA M_v}{2000}, \quad (2)$$

where M_v is the ratio of solid mass to pore fluid volume (g/cm^3).

3. Results

As TEOS polymerizes, it is unclear at what point the polymer becomes a ‘surface’ (from an NMR viewpoint). Relaxation measurements for TEOS monomer in ethanol and of the precursor sol after the hydrolysis step indicate no surface area. Surface area versus reaction time of the condensation step for duplicate B2 growth experiments are presented in fig. 2. Care must be taken in interpreting these results, since two variables (i.e., the fraction of silicon species which appear as a surface and the specific surface area of those species) are changing with time. Upon introduction of the base catalyst the solids content (which is required for determining surface area) will increase approaching the final value of

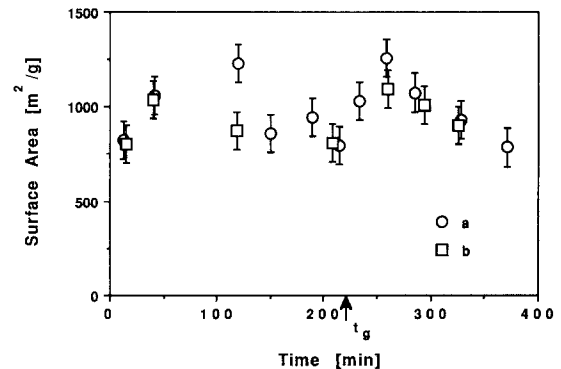


Fig. 2. Variation of surface area versus time after addition of base for a two-step acid–base-catalyzed process. The gel time is indicated by t_g (a and b are duplicate samples).

0.14 g/cm³. The solids content is assumed to equal the final value of 0.14 g/cm³ to allow calculation of intermediate surface areas. This point deserves further discussion since the solids content is not the mass per volume of the gel spanning cluster but rather, the mass of TEOS (on a silica weight basis) which has sufficiently polymerized to appear as surface. The effect of this assumption is that the specific surface area (i.e., the surface area of the solid phase) will be overpredicted. However, the results of fig. 2 are interesting in the sense that the surface area appears in a short time after the base and water is added ($t/t_g < 0.1$) and remains essentially constant throughout the gelation process. Although polymerization and condensation reactions occur even after the gel point, the molecular weights of most condensed silicon species may be sufficient to appear as surface and solids in these NMR measurements. These surface area values are of the same order (800 to 1000 m²/g) as observed for B2 gels aged in ethanol for very long times [16] and for B2 xerogels (from nitrogen adsorption) [21]. Thus, although significant chemical and physical changes continue during gelation and aging in mother liquor, they seem to have little net effect on surface area.

For producing monolithic xerogels (or as a prelude to aerogel synthesis) an aging step may be employed where the gel is aged, often at elevated temperature, in its mother liquor (for B2 a mixture of ethanol, water, base and partially reacted TEOS) prior to drying. This allows the gel matrix to strengthen via syneresis, condensation and dissolution/reprecipitation [2] so the gel can better withstand the high capillary forces associated with the final stages of drying. Scherer [22] attributed the increase in modulus of wet B2 gels to a reduction in porosity and a stiffening of the solid matrix. The effect of aging time on the wet pore size distribution (PSD) of B2 silica gel (15 wt% solids) is illustrated in fig. 3. The gel is aged in its mother liquor at 303 K and the NMR experiments are performed at the same temperature. The time required for the NMR pore size analysis is small (5 min) as compared to the aging times studied. PSD are presented as $dV/d(\log r)$ plots so that the integrated area under the plot

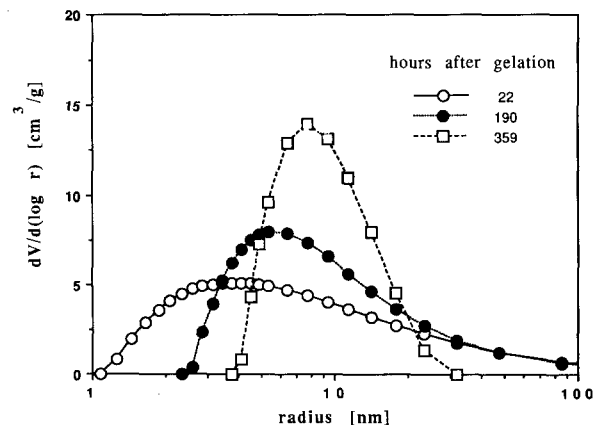


Fig. 3. Pore size distributions as a function of aging time for a B2 gel aged in mother liquor at 303 K (lines are linear interpolations).

directly corresponds to the pore volume. Since the sample did not exhibit microporosity, integration of the curves in fig. 3 indicates that the total mesopore volume is approximately constant during aging for the times studied. Optical observation of the sample indicated little shrinkage.

To increase the rates of condensation, syneresis, and coarsening that in combination contribute to strengthen the gel matrix and hence, shorten aging times, gels may be aged at elevated temperatures [2]. The effect of increased temperature on pore size distribution is illustrated in fig. 4. To perform the NMR measurements, samples were quickly cooled from 333 to 303 K, allowed

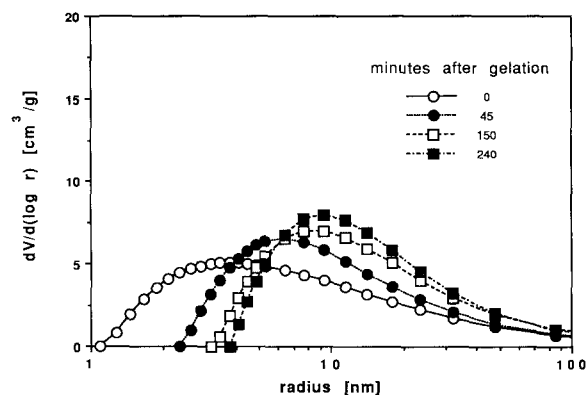


Fig. 4. Pore size distributions as a function of aging time for a B2 gel aged in mother liquor at 333 K (lines are linear interpolations).

to equilibrate before analysis (~ 30 min) and then reheated to 333 K after the PSD analysis. The samples were all analyzed at 303 K to minimize uncertainty resulting from the temperature dependence of the NMR α and β parameters. After only 150 min at 333 K, the mean pore size increases by a factor of two over that of the 303 K sample aged for 359 h and the PSD narrows similarly despite an aging time nearly two orders of magnitude shorter. This could be attributed to an increase in the rates of monomer hydrolysis, condensation, syneresis or coarsening. The reduction of smaller pores and increase in mean pore size suggests that coarsening is the predominant aging process affecting PSD. As aging continues, the matrix stiffens [7] and the modulus increases [22] hindering further pore structure change, causing the 150 and 240 min samples to appear similar.

The effect of solids content on the wet gel PSD during temporal aging is illustrated in fig. 5. In general, the narrowing of the PSD with time is independent of solids content as both 15 and 30 wt% exhibit similar broad distributions after 22 h at 303 K that narrow after an extended time (~ 2 weeks). Hence narrowing is not limited by rearrangement or shrinkage processes that would be inhibited by the greater solids concentration in the 30 wt% samples. As expected from the measured solids content, the area under the curve (i.e., the total pore volume) decreases with in-

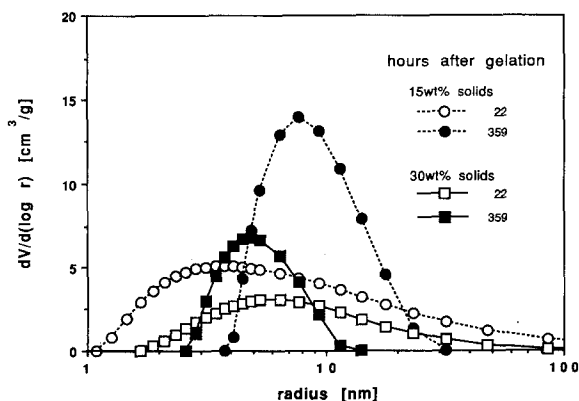


Fig. 5. Pore size distributions as a function of solids content and aging time for B2 gels aged in mother liquor at 303 K (lines are linear interpolations).

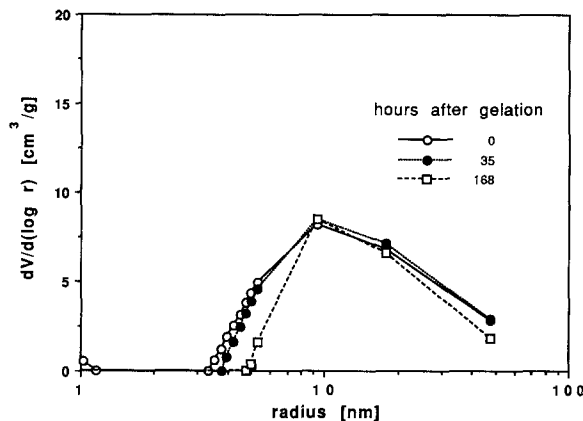


Fig. 6. Pore size distributions as a function of aging time for an A2 gel aged in mother liquor at 303 K (lines are linear interpolations).

creasing solids content and aging appears to favor a smaller mean pore size with increasing solids content.

The two-step acid–base-catalyzed 15 wt% silica gel (B2) was selected as our reference material, since this particular silica gel has been studied previously by several investigators [2,14,19]. At the gel point, B2 contains unhydrolyzed monomer, and, since it is prepared at $\text{pH} \approx 8$, the rates of condensation, syneresis and coarsening are high. For comparison we present in fig. 6, PSDs of a two-step acid-catalyzed gel prepared near the isoelectric point of silica ($\text{pH} \approx 2$) during aging at 303 K. Over the time period studied (~ 1 week), the pore size distribution was essentially constant.

4. Discussion

By measuring pore structure during aging, we have shown that both a narrowing of pore size distribution and an increase in mean pore size is obtained when a two-step acid–base-catalyzed silica gel is aged in its mother liquor. Although syneresis is expected for these gels, these samples were cast in 5 mm glass NMR tubes and the gel appeared to adhere to the walls of the tubes which could retard the effects of syneresis. However, since syneresis is a function of sample size

as well as aging conditions [5], no attempt was made to isolate the effects of syneresis and hence, coated tubes were not employed to enable syneresis. With increased aging temperature/time, a higher degree of condensation, and increased coarsening via dissolution/reprecipitation will result. This will lead to greater mechanical strength and a larger mean pore size, thus allowing greater drying rates without fracture. Our results show that aging at 303 K results in an increase in the mean pore size and a narrowing of the PSD. Both of these effects will allow faster drying rates without cracking since stress and stress gradients during drying will be reduced. By increasing the aging temperature from 303 to 333 K, the rate of this pore size narrowing process is increased in excess of an order to magnitude.

The observed factor of two decrease in mean pore size with a doubling of the solids content is consistent with our finding that the surface area is essentially independent of aging time or solids content. Since we measure the distribution of hydraulic radii (proportional to volume/surface area), one would expect the mean pore size for these samples to be inversely proportional to pore volume if the surface area is constant.

In contrast to the B2 gels, little change occurs for acid-catalyzed gels when aged at 303 K for similar time periods. The lack of change in pore structure with aging for the acid-catalyzed gel (A2) is presumably a result of several factors: (1) there is no monomer available at the gel point; (2) the rate of silica dissolution (to produce soluble silica) is low, causing the coarsening rate to be low; (3) since the aging is carried out near the IEP of silica, the rates of condensation and syneresis are low. These combined factors lead to little alteration of the pore morphology during aging.

5. Conclusions

Using low field NMR relaxation measurements of pore fluid in a two-step acid-base-catalyzed silica gel, we have shown that the pore size distribution in the wet state is significantly altered by employing various aging techniques. The

mean pore size increased and the width of the pore size distribution decreased for gels aged at 303 K over a period of several weeks. By employing a higher aging temperature of 333 K, the kinetics of this pore structure change were increased by one to two orders of magnitude because of a higher degree of condensation and increased coarsening via dissolution/reprecipitation. However, temporal and thermal aging of a two-step acid-acid-catalyzed silica gel had little effect on the wet-gel pore structure.

This work has been supported by Sandia National Laboratories (#05-5795). One of the authors, P.J.D., has been partially supported by a New Mexico Fellowship for Underrepresented Groups in Science. The authors thank G. Johnston of University of New Mexico/NSF Center for Micro-Engineered Ceramics for performing nitrogen adsorption analysis used in the β determination and Dr G.W. Scherer of DuPont for his many helpful discussions.

References

- [1] R.K. Iler, *The Chemistry of Silica* (Wiley, New York, 1979).
- [2] C.J. Brinker and G.W. Scherer, *Sol-Gel Science* (Academic Press, New York, 1989).
- [3] G.W. Scherer, *J. Non-Cryst. Solids* 108 (1989) 18.
- [4] L.L. Hench and J.K. West, *Chem. Rev.* 33 (1990).
- [5] G.W. Scherer, *J. Non-Cryst. Solids* 108 (1989) 28.
- [6] T.P. Ponomareva, S.I. Kontorovich, N.I. Chekanov and E.D. Schukin, *Kolloidn. Zh.* 46 (1984) 118.
- [7] Z.Z. Vysotskii and D.N. Strazhesko, in: *Adsorption and Absorbents*, No. 1, ed. D.N. Strazhesko (Wiley, New York, 1973) p. 55.
- [8] Y. Klimentova, L.F. Kirichenko and Z.Z. Vysotskii, *Ukr. Khim. Zh.* 36 (1970) 56.
- [9] J.F. Quinson, N., Tchiphkam, J. Dumas, C. Bovier, J. Serughetti, C. Guizard, A. Larbot and L. Cot, *J. Non-Cryst. Solids* 99 (1988) 151.
- [10] C.J. Brinker, K.D. Keefer, D.W. Schaefer, R.A. Assink, B.D. Kay and C.S. Ashley, *J. Non-Cryst. Solids* 63 (1982) 45.
- [11] G. Scherer, *J. Non-Cryst. Solids* 109 (1989) 183.
- [12] M. Brun, A. Lallemand, J. Quinson and C. Eyraud, *Thermochim. Acta* 21 (1977) 59.
- [13] J.F. Quinson, J. Dumas and J. Serughetti, *J. Non-Cryst. Solids* 79 (1986) 379.
- [14] D.P. Gallegos, K. Munn, D.M. Smith and D.L. Stermer, *J. Colloid Interface Sci.* 119 (1987) 127.

- [15] J.A. Brown, L.F. Brown, J.A. Jackson, J.V. Milewski and B.J. Travis, Proc. SPE/DOE Unconventional Gas Recovery Symposium, 201 (1982).
- [16] C.L. Glaves, C.J. Brinker, D.M. Smith and P.J. Davis, Chem. Mater. 1 (1989) 34.
- [17] B. Ewing, P.J. Davis, P.D. Majors, G. Drobney, D.M. Smith and W.E. Earl, J. Am. Ceram. Soc., in press.
- [18] C.J. Brinker, K.D. Keefer, D.W. Schaefer and C.S. Ashley, J. Non-Cryst. Solids 48 (1982) 47.
- [19] D.P. Gallegos and D.M. Smith, J. Colloid Interface Sci. 122 (1988) 143.
- [20] K.R. Brownstein and C.E. Tarr, J. Magn. Reson. 26 (1977) 17.
- [21] P.J. Davis, D.P. Gallegos and D.M. Smith, Pow. Tech. 53 (1987) 39.
- [22] G.W. Scherer, J. Non-Cryst. Solids 109 (1989) 183.